A&A 484, 311–315 (2008)
DOI: 10.1051/0004-6361:200809374

Astronomy & Astrophysics

The Seyfert 1 Galaxy Mrk 335 at a very low flux state: mapping the soft X-ray photoionised gas

A. L. Longinotti, A. Nucita, M. Santos-Lleo, and M. Guainazzi

ESAC – European Space Astronomy Centre, PO Box 78, 28691 Villanueva de la Cañada, Madrid, Spain
e-mail: alonginotti@sciops.esa.int

Received 9 January 2008 / Accepted 7 March 2008

ABSTRACT

Context. This paper reports on an XMM-Newton observation of the Seyfert 1 Galaxy Mrk 335 performed as a target of opportunity when the source was in an unusually low flux state.
Aims. The low level of continuum emission unveiled an underlying line-rich soft X-ray spectrum, which can be studied with the Reflection Grating Spectrometer.
Methods. The emission features were analysed at high resolution with unprecedented detail for this source. Line ratio diagnostics from H-like and He-like ions indicate that the line emission arises in X-ray photoionised plasma. Extensive simulations were performed with the CLOUDY photoionisation code. The physical properties of the line emitting material were derived from the comparison of the expected and observed line intensities.
Results. Because of the degeneracy in the ionisation parameter, a number of different solutions for the electron density and column density of the gas are consistent with the spectral diagnostics. This prevents us from uniquely determining the properties of the plasma; however, the location(s) of the X-ray photoionised gas can be constrained to within 0.06 pc (outer boundary). This limit places the X-ray line emitting gas at the inner edge of the material where the broad optical lines are produced (broad line region).

Key words. galaxies: active – galaxies: individual: Mrk 335 – X-rays: galaxies

1. Introduction

The soft X-ray spectrum of Seyfert galaxies has represented for astronomers a region of great interest and, at the same time, a sort of challenge. With the advent of high-resolution spectrometers onboard *XMM-Newton* and *Chandra*, it has been possible to reveal the nature of emission in this spectral band at least in obscured sources (Guainazzi & Bianchi 2007, and references therein). Many authors concur to indicate that the origin of the soft X-ray emission in these sources is caused by photoionisation of extended circumnuclear gas on kpc scale irradiated by the active nucleus which produces He and H-like transitions of heavy elements and L-shell transitions from Fe (e.g. NGC 1068, Kinkhabwala et al. 2002; Mrk 3, Bianchi et al. 2005, NGC 4151, Armentrout et al. 2007, to cite the most outstanding cases).

On the other hand, the scenario for unobscured AGN is not so definite. The lack of line-of-sight obscuring material in this type of sources, allows the whole nuclear radiation to escape unblocked to the observer, so that the soft X-ray spectrum is dominated by a smooth excess of continuum rather than features from reprocessed material (Piconcelli et al. 2005; Crummy et al. 2006).

In about half of the Seyfert 1 galaxies (Crenshaw et al. 2003; Blustin et al. 2005), the presence of intervening ionised gas is directly observable as a series of absorption features, which present velocity shifts when originating in outflowing or inflowing gas. For the sources studied with the longest integration times, it has been possible to place some constraints on the electron density of the gas and, consequently, on the distance of these warm absorbers, mainly through variability studies. The emerging picture is far from being a homogeneous description of the circumnuclear ionised gas. Among many cases, we recall that the distance of the absorber(s) in NGC 3783 was estimated to be 1–3 pc from the nucleus (Netzer et al. 2003; Behar et al. 2003), whereas it was found to be consistent with subparsec scale in NGC 3516 (Netzer et al. 2002) and it was estimated to be within 4 light days from the nucleus in NGC 4051 (Krongold et al. 2007).

Mrk 335 is a Seyfert 1 galaxy ($z = 0.026$) with a long X-ray history, since it has been observed by almost all X-ray observatories in the past. *EXOSAT* (Turner & Pounds 1989) and *BBXRT* (Turner et al. 1993a) revealed the presence of an excess of emission in the soft X-rays band, later confirmed in *ASCA* data by Reynolds (1997). No clear evidence of warm absorption was established (Reynolds 1997; George et al. 1998), but *ROSAT* data tentatively suggested spectral complexity in the soft X-ray (Turner et al. 1993b). Nandra & Pounds (1994) found evidence of a hard X-ray edge in the *Ginga* data. The presence of the Compton reflection component and a strong Fe Kα line was revealed in *BeppoSAX* data (Bianchi et al. 2001) and later confirmed in *XMM-Newton* observations (Gondoin et al. 2002; Longinotti et al. 2007; O'Neill et al. 2007). In 2006 the source was observed by the *Suzaku* satellite (Larsson et al. 2007). The spectrum was characterised by a strong soft excess and a reflection component, closely resembling the *XMM-Newton* data; but despite the availability of the high-energy data up to 40 keV, it has not been possible to model the broadband spectrum unambiguously. In May 2007, *Swift* caught Mrk 335 in a historical low X-ray flux state, with an extremely hard X-ray power law above 2 keV (Grupe et al. 2007). Following this discovery, the source was observed again by *XMM-Newton* in July 2007 as a target

Table 1. Observation Log of Mrk 335 as observed by *XMM-Newton*.

OBSID	Date	RGS exp	pn exp	Γ_{soft}	$Flux_{0.3-2}$	Γ_{hard}	$Flux_{2-10}$
–	(dd/mm/yyyy)	(ks)	(ks)	–	(10^{-12} erg cm^{-2} s^{-1})	–	(10^{-12} erg cm^{-2} s^{-1})
0510010701[a]	10/07/2007	22	15	2.84 ± 0.03	1.95 ± 0.04	1.02 ± 0.07	$3.34^{+0.23}_{-0.10}$
0306870101[b]	03/01/2006	130	92	2.72 ± 0.01	32.16 ± 0.04	2.09 ± 0.01	17.72 ± 0.07
0101040101[c]	25/12/2000	34	30	2.80 ± 0.01	31.74 ± 0.06	2.16 ± 0.02	15.00 ± 0.02

[a] Grupe et al. (2008), [b] O'Neill et al. (2007), [c] Longinotti et al. (2007). The X-ray properties have been measured from the pn spectra.

of opportunity (ToO) (Grupe et al. 2008). This paper reports on the high-resolution spectrum obtained by the Reflection Grating Spectrometer (RGS) onboard *XMM-Newton*.

2. Observation and data reduction

Mrk 335 was observed by *XMM-Newton* on 10 July 2007 (OBSID 0510010701) for a duration time of 25 ks. Data from the three instruments EPIC (0.3–10 keV), RGS (5–38 Å), and Optical Monitor (OM, 6 filters in the 1800–6000 Å bandpass) were available (Struder et al. 2001; Den Herder et al. 2001; Mason et al. 2001). The detailed analysis of EPIC and OM data will be published in Grupe et al. (2008). In this paper, only the RGS data from the ToO observation are considered. However, Table 1 reports the broadband properties from all the three *XMM-Newton* available data sets to allow the reader an immediate comparison among the flux states of this source. The raw data were processed with SAS 7.1.0 with the task `rgsproc` for the RGS data, which produces spectral products for the source and the background and response matrices. No background flares due to high-energy particles are present in this observation. For the OM data, we decided to extract the magnitudes and fluxes from the pipeline products (PPS).

3. RGS spectral analysis

The spectral analysis was performed using the fitting package SPEX[1] (ver. 2.0), simultaneously fitting both spectra from the two RGS cameras. A preliminary analysis was carried out using the first-order spectra, re-binned according to the resolution of the instrument and with a signal-to-noise ratio of 5 over the whole 5–38 Å range. This binning was used only to test the agreement between the power-law slopes of the RGS and of the EPIC data and to visually check for the presence of broad features in the spectrum (Fig. 1). Otherwise, since many spectral channels fall in the limit of low number of photons, the unbinned spectrum was used for the spectral analysis and the C statistic was applied (Cash 1979). The quoted errors correspond to the 1σ level (i.e. $\Delta C = 1$, for one interesting parameter). Galactic absorption of column density $N_{\rm H} = 3.9 \times 10^{20}$ cm^{-2} is included in all the models (Dickey & Lockman 1990).

At first glance, the RGS spectrum of Mrk 335 appears to be characterised by a weak continuum and a number of emission features (Fig. 1). The continuum has been fitted with a power law with $\Gamma = 2.75 \pm 0.17$, in agreement with the slope measured by the pn instrument (Table 1). All the transitions listed in Table 2 have been included in the model to fit the narrow emission lines in the spectrum. Each line was fitted with a delta line model, fixing the centroid energy to the laboratory values. Lines fluxes are reported in Table 2. All but two lines, for which only upper limits are found, yield an improvement in the fit higher

[1] http://www.sron.nl/divisions/hea/spex/version2.0/release/index.html

Table 2. Fluxes of the soft X-ray lines found in the RGS spectrum.

Transition	λ (lab)	$Flux^1_{FWHM=0}$	ΔC	$Flux^2_{FWHM(OVIII)}$
–	(Å)	ph m^{-2} s^{-1}	–	ph m^{-2} s^{-1}
FeXVII	17.073	<0.05	$\Delta C = 1$	0.06 ± 0.04
OVII Heβ	18.627	<0.03	$\Delta C = 0$	0.06 ± 0.04
OVIII Lyα	18.969	0.20 ± 0.04	$\Delta C = 31$	0.27 ± 0.05
OVII Heα (r)	21.600	0.10 ± 0.06	$\Delta C = 4$	0.17 ± 0.08
OVII Heα (i)	21.790	0.26 ± 0.08	$\Delta C = 21$	0.31 ± 0.09
OVII Heα (f)	22.101	0.17 ± 0.07	$\Delta C = 12$	0.16 ± 0.07
NVII Lyα	24.781	0.13 ± 0.05	$\Delta C = 12$	0.18 ± 0.05
CVI Lyβ	28.446	0.13 ± 0.06	$\Delta C = 13$	0.20 ± 0.07
CVI Lyα	33.736	0.15 ± 0.06	$\Delta C = 8$	0.24 ± 0.07

1) Line width fixed to $FWHM = 0$; 2) line width fixed to $FWHM = 2200$ km s^{-1}. The energy centroids were fixed to the laboratory value in both cases. The column with the improvement in terms of ΔC refers to the detection significance for the fit with the zero-width lines.

or equal to $\Delta C = 4$, corresponding to 95.4% for one free parameter. The final fit statistic including all transitions in Table 2 is C-statistic = 6247 for 5264 degrees of freedom (d.o.f.). As a second step, we checked for the presence of the radiative recombination continua (RRC) from CV, NVII, OVII, and OVIII at $\lambda = 31\,622, 18\,587, 16\,771$, and $14\,228$ Å, which are visible in the binned spectrum. They were incorporated in the model, but when this is fitted, only upper limits on the emission measures could be found, so they are not considered in the following. A careful visual inspection of the spectrum did not reveal any absorption feature.

The detected lines were then checked for line broadening. The OVIII Lyα line is the most intense isolated transition in the spectrum, and it is not affected by bad pixels. A Gaussian profile was fitted to this line with the wavelength frozen to the expected value of 18.96 Å and the width free to vary. The measured line $FWHM$ is $\sigma = 0.14 \pm 0.05$ Å. We fitted all the spectral lines fixing their $FWHM$ to the value corresponding to the one of the OVIII Lyα, obtaining the fluxes reported in the third column of Table 2. The spectrum was also checked for line shifts by leaving the centroids of the strongest transitions free to vary. For the OVIII Lyα line, a blueshift of $\Delta\lambda = -0.014 \pm 0.013$ Å is found, with an improvement of $\Delta C = 7$. For the OVII intercombination line the 90% limits on the shift with respect to the laboratory wavelength are +0.018 and –0.054 Å. Taking into account that the present signal-to-noise ratio does not allow us to distinguish line contamination and that the RGS systematic error of 8 mÅ is included in the error estimate, we conclude that the peak wavelengths are consistent with the laboratory values.

3.1. A close look at the H-like and He-like emission lines in the spectrum

The spectral fit in the previous section and the fluxes reported in Table 2 reveal that the OVII triplet is characterised by dominant

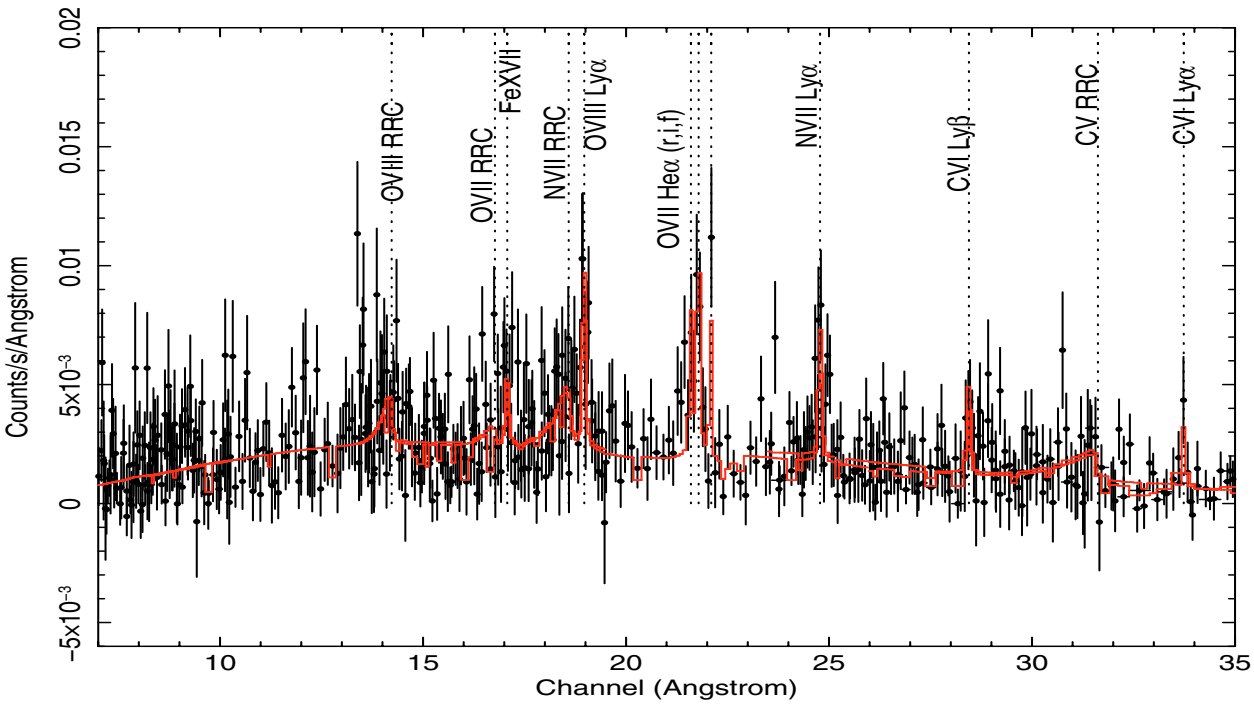

Fig. 1. The RGS spectrum of Mrk 335 (corrected for the source redshift). The fitted model, plotted as a red line, consists of a power law with $\Gamma \sim 2.7$ and the emission features reported in Table 2. The data have been binned according to the instrumental resolution only for plotting purposes (see text).

intercombination line emission and weaker resonant and forbidden lines (see Fig. 2 for a zoom on this spectral portion). The line ratios in He-like ions provide a powerful diagnostic of the physical properties of the emitting gas, mainly by indicating whether the X-ray lines are produced by collisional plasma, by photoionisation, or in a hybrid environment (Porquet & Dubau 2000; Porter & Ferland 2007). The lines ratios from the present spectra were calculated with the OVIII Lyα and the OVII triplet lines. The numbers estimated are $\frac{\mathrm{OVIII\ Ly}\alpha}{\mathrm{OVII}(f)} = 1.17 \pm 0.53$, $G = \frac{(f+i)}{r} = 4.30 \pm 2.70$, $L = \frac{r}{i} = 0.38 \pm 0.25$, and $R = \frac{f}{i} = 0.65 \pm 0.33$, where r, i, f indicate the intensity of the resonant, intercombination, and forbidden line components in the triplet. Given the high value of the G ratio, albeit measured here with considerable uncertainties, the reported line ratios are consistent with an origin in photoionised gas and a possible contribution from collisional processes (Porquet & Dubau 2000).

Extensive simulations were run through the photoionisation code CLOUDY (Ferland et al. 1998) in order to constrain the physical properties of the emitting gas. The aim of these simulations was to extract the expected theoretical values for the line fluxes and to compare them to the observed fluxes. In addition to the line ratios cited above, we also consider the following ratios: $\frac{\mathrm{CVILy}\alpha}{\mathrm{OVIIILy}\alpha} = 0.75 \pm 0.33$, $\frac{\mathrm{CVILy}\beta}{\mathrm{OVIIILy}\alpha} = 0.65 \pm 0.33$, $\frac{\mathrm{NVIILy}\alpha}{\mathrm{OVIIILy}\alpha} = 0.65 \pm 0.28$, and $\frac{\mathrm{CVILy}\beta}{CVILy\alpha} = 0.86 \pm 0.53$. These line ratios were calculated assuming the fluxes from the first column in Table 2 i.e. assuming lines with a delta profile. The fluxes measured with non zero-width Gaussian profiles are nonetheless consistent with this estimate.

The theoretical line fluxes were calculated assuming the spectral energy distribution (SED) of a standard AGN as

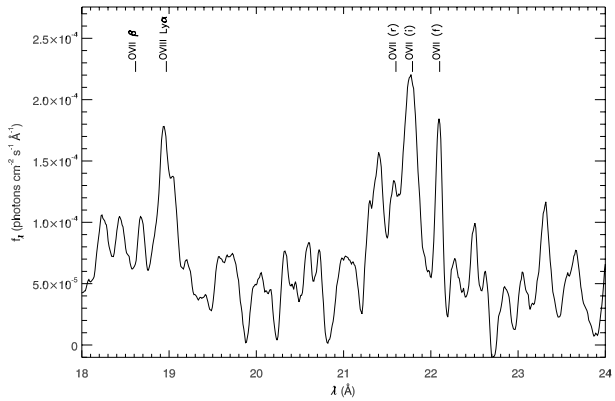

Fig. 2. Zoom of the RGS spectrum in the energy range containing the emission lines from oxygen.

calculated by Korista et al. (1997). The treatment of the UV radiation field is particularly important when dealing with a high ratio between the intercombination and the forbidden lines. In fact, an intense UV source can provide enough photons to depopulate the forbidden level 2 ^{3}S via photo-excitation and then pump the electrons into the intercombination level 2 ^{3}P, resulting in a more intense intercombination line (Mewe & Schrijver 1978; Kahn et al. 2001). We therefore compared the observed SED of Mrk 335 to the one assumed by CLOUDY. The UV spectrum as observed by the *XMM-Newton* Optical Monitor is in good agreement with the SED by Korista et al. (1997). The spectral slope of the UV-X-ray power-law commonly defined as $\alpha_{\mathrm{ox}} = -0.3838 \log\left[\frac{F_\nu(2\ \mathrm{keV})}{F_\nu(2500\ \text{Å})}\right]$ was estimated using the pn and OM fluxes at 2 keV and at 2340 Å, respectively giving $F_{2\ \mathrm{keV}} = 0.53 \times 10^{-11}$ erg cm^{-2} s^{-1} keV^{-1} and $F_{2340} = 2.5 \times 10^{-14}$ erg cm^{-2} s^{-1} Å^{-1}. The resulting UV-X-ray power

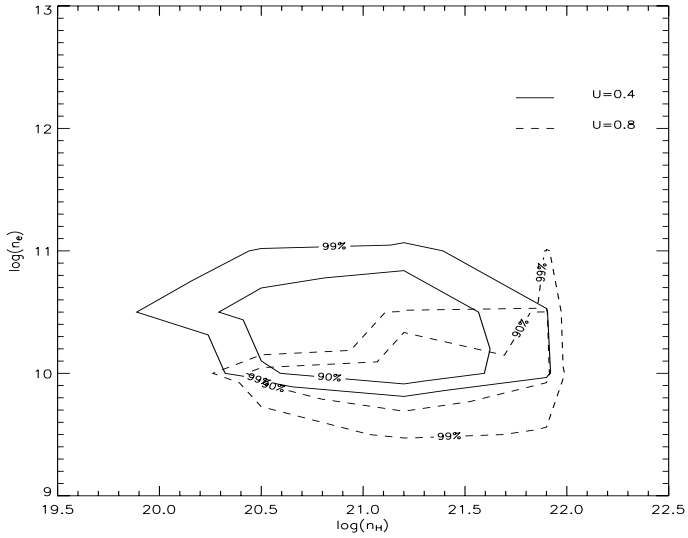

Fig. 3. Contour plots for electron and column density of the line emitting gas. The contours were obtained by comparing the ratios of the emission lines listed in Table 2 to the values predicted by CLOUDY simulations (see text for details). The curves define the 90 and 99% regions in the parameters space for *for all the eight line ratios*. Only those values of the ionisation parameter yielding a valid solution have been plotted. The corresponding physical quantities are listed in Table 3.

law $\alpha_{ox} = -1.32$ is fully consistent with the average Seyfert value assumed by CLOUDY, i.e. $\alpha_{ox} \sim 1.4$.

The simulations were carried out by varying the column density of the gas N_H and ionisation parameter U[2] over a range of electronic density n_e spanning 10^6 to 10^{14} cm^{-3}. These quantities were varied in small steps, so that a fine grid of possible solutions was obtained. In particular, the ionisation parameter is stepped between log $U = -2$ and log $U = 2$.

To compare the measured line ratios to the spectral model simulated by CLOUDY, each line ratio was searched over the grid of predicted values in the following way. For each line ratio i the observed value $L_{o,i}$ with its error err($L_{o,i}$) and the corresponding theoretical value $L_{t,i}$ have been taken into account and used to calculate the quantity $\sigma_i^2 = \dfrac{(L_{o,i} - L_{t,i})^2}{\mathrm{err}(L_{o,i})^2}$

Then, the quantity $(\sum\sigma_i^2)^{1/2}$ has been minimised, i being the summation index over the considered line ratio. The contour plots in the N_h–n_e plane have been drawn by imposing a distance equal to 4.61 and 9.21 from the minimum solution, corresponding to 90 and 99% levels of confidence. The inner and outer contours in Fig. 3 therefore represent the locii of valid solutions distributed respectively at 90 and 99% considering the eight line ratios simultaneously.

The measured data points are consistent only with CLOUDY solutions in the range log $U = 0.4$–0.8, corresponding to the continuous and dashed lines in Fig. 3. Since one of the output of CLOUDY is the column density of the gas, an estimate of the size of the emitting material l was provided using the relation $l = N_H/n_e$. For each solution, the distance r_0 of the cloud from

[2] U is defined as $\dfrac{\phi(\mathrm{H})}{n_e\, c}$ where the radiation field is expressed by $\phi(\mathrm{H}) = \dfrac{k}{4\pi\, r_0^2}\displaystyle\int_{\nu 1}^{\nu 2} \frac{\pi\, F_\nu}{h\nu}\mathrm{d}\nu$ with $\nu 1 = 1$ Ryd and $\nu 2 = \infty$ and the relation between the normalisation costant k, and the bolometric luminosity of the source is expressed by $L = k\displaystyle\int_{\nu 1}^{\nu 2} \pi F_\nu \mathrm{d}\nu$.

Table 3. Summary of the physical properties of the gas clouds estimated from the 99% contour plot in Fig. 3.

log U –	n_e range cm^{-3}	n_H range cm^{-2}	*dist range* cm	*size range* cm
0.4	$10^{9.8-11.1}$	$10^{19.9-21.9}$	$1.95 \times 10^{16-17}$	10^{8-12}
0.8	$10^{9.5-11}$	$10^{20.3-22}$	$1.95 \times 10^{16-17}$	10^{9-13}

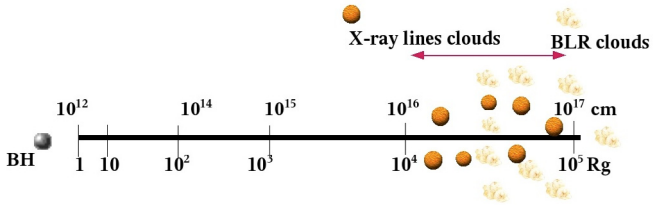

Fig. 4. The cartoon shows qualitatively the location of the ionised gas in the nucleus of Mrk 335 on a scale of gravitational radii and the corresponding cm scale.

the ionising source can be extracted from CLOUDY by replacing the AGN bolometric luminosity in the definiton of the ionisation parameter given above. The value $L_{bol} = 10^{44.7}$ erg s^{-1} was adopted after Woo & Urry (2002). For each ionisation parameter U, the values of the distance of the emitting gas cloud(s) from the nucleus and its size have been estimated. The minimum and maximum values correspond to the 99% contour for the range in electron and column density of the gas in Fig. 3. The solutions admitted by our data are summarised in Table 3 and they will be discussed in the following section.

4. Discussion

The RGS spectrum of Mrk 335 at low state provides a unique opportunity for getting insights into an X-ray reprocessing region that is not easily accessible in Seyfert 1 objects. The soft X-ray emission lines could be observed because of the decrease in the continuum flux. The nuclear power was attenuated for reasons as yet unknown, however the most straightforward explanation could be partial obscuration of the central source. At first glance, this object seems to be analogous to the other well-known case of an extremely variable Seyfert 1, NGC 4051, which showed a very rich emission line spectrum when it was observed in a low flux state by *XMM-Newton* (Pounds et al. 2004). According to these authors, the analysis of the emission lines in this source, especially of the OVII triplet, pointed to interpret the soft X-ray spectral features as arising from photoionised low-density gas distributed on a large scale, consistent with the AGN narrow line region. The variability history of Mrk 335 and the comparison with other variable AGN are not the prime focus of the present paper. However, the similarity between NGC 4051 and Mrk 335 suggests to consider first the geometry of the system.

Mrk 335 is a pure Seyfert 1 galaxy, since the nuclear emission does not suffer *any* obscuration nor does absorption when the source is observed at high state, as shown by previous, recent X-ray observations (Longinotti et al. 2007; O'Neill et al. 2007). Nonetheless, the low-state, soft X-ray spectrum resembles the RGS spectra recently observed in obscured AGN by Guainazzi & Bianchi (2007). It is then reasonable to postulate that we are observing the same line-emitting gas in Mrk 335 as became observable due to the drop in the continuum flux. There

are some objections to this hypothesis. The main point is that, in many obscured sources, the soft X-ray photoionised matter was demonstrated to be coincident with the extended narrow line region, i.e. well out of the obscuring torus (Bianchi et al. 2006). The scale of this gas is much larger than the distance of the emitter observed in Mrk 335 for all the possible solutions listed in Table 3. For this reason, the hypothesis of a common location of the soft X-ray photoionised gas for unobscured and obscured objects is discarded in the present case.

The simulations run with CLOUDY cannot uniquely constrain the ionisation parameter or the electron density of the gas, and yet they provide a range of physical conditions for the gas that are noticeably in agreement. The distance of the photoionised plasma from the nuclear source ranges approximately from 7 to 77 light days, meaning that the gas is always confined within ∼0.06 pc. The column density never gets higher than 10^{22} cm^{-2} (see contours in Fig. 3) and the size of the emitting region(s) always appears quite small, the dimension of the largest cloud being $\sim 10^{11}$ cm. From the black hole mass $M = 14.2 \pm 3.7 \times 10^6\ M_\odot$ (Peterson et al. 2004), the Schwarzschild radius R_s is estimated to be around 4×10^{12} cm. The distance of the Broad Line Region (BLR) from the central source can be found by considering the width of the optical lines and assuming that the BLR gas is virialised. The Hβ *FWHM* was measured by Boroson & Green (1992), and it is equal to 1640 km s^{-1}, in agreement with the reverberation mapping measurements provided by (Peterson et al. 2004). The BLR can then be located at $\sim 7 \times 10^{16}$ cm, and that this gas in Mrk 335 is constituted of several clouds of emitting material forming a clumpy medium was suggested by Arav et al. (1997) on the basis of observational constraints.

It is very likely that the X-ray photoionised gas is inner to the BLR clouds and it is also reasonable that the two materials form a continuous distribution of clouds. One can imagine that the innermost clouds spread out towards the nucleus, reaching an ionisation level high enough to emit the observed soft X-ray lines. In this case, the spectral line should suffer line broadening due to the vicinity of the central black hole, although this effect should not be extreme because the Schwarzschild radius is 3 orders of magnitude smaller. The Gaussian line width measured in the OVIII Lyα corresponds to a *FWHM* of 2200 ± 750 km s^{-1}. We checked for the width in the OVII intercombination line, and the upper limit on the line width is consistent with the measurement from the OVIII Lyα at <0.15 Å. The distance estimated from the virial assumption is then constrained within $\sim 2.3 \times 10^{16}$ cm and 1.2×10^{17} cm. In principle, this value can be easily reconciled with the distance inferred from CLOUDY; on the other hand, it may add an independent observational constraint on the structure of the gas. In fact, the underlying assumption in our CLOUDY model is that all the X-ray emission lines originate in the same cloud, therefore the distances in Table 3 must refer to the bulk of the photoionised gas. The distance estimated from the OVIII Lyα width may indicate that the spectral lines come from a distribution of clouds and that OVIII is only concentrated in the innermost ones. To conclude, the X-ray photoionised gas is likely to be located within the optical BLR, as depicted qualitatively in Fig. 4. Longer exposures of this AGN at a serendipitous low state are needed to reach firm conclusions.

Finally, it has to be remarked that the existence of circumnuclear ionised gas in the innermost region is not a novelty in this AGN. Longinotti et al. (2007) reported on the detection of a narrow absorption feature around 5.9 keV in the EPIC spectrum of the 2000 observation (see Table 1). This feature was identified as a redshifted Fe XXVI Kα transition and interpreted as the signature of gas inflowing towards the nucleus at a velocity of 0.11–0.15 *c*. Six years later, *XMM-Newton* observed the source again; the detection of an *emission* line at ∼7 keV in the EPIC spectrum was associated to the presence of highly ionised material on a distance scale much larger than those discussed herein (O'Neill et al. 2007). Interestingly, the most recent X-ray observations of Mrk 335 performed during the past year by *Suzaku* and *XMM-Newton* did not show any emission line at 7 keV (Larsson et al. 2007; Grupe et al. 2008), implying that rapid line variability must be involved. The potential physical connection among the briefly outlined observational results and the soft X-ray lines in the present work should be a point of major interest in the next studies of this intriguing active galaxy.

Acknowledgements. This paper is based on observations obtained with XMM-Newton, an ESA science mission with instruments and contributions directly funded by ESA Member States and NASA. The authors wish to thank the XMM-Newton Project Scientist Norbert Schartel for coordinating the observation and the release of the *XMM-Newton* data. We are grateful to many people within the XMM Science Operation Centre: Pedro Rodriguez-Pascual for his contribution on Mrk 335 Optical/UV SED, Andy Pollock for always being a wise advisor on the RGS data treatment, and Maria Diaz-Trigo for support with the use of the SPEX software. The authors thank R. Porter for help with CLOUDY simulations. We thank Dirk Grupe for a fruitful exchange of opinions on the XMM-Newton data, and we warmly thank Yair Krongold for many stimulating discussions on this paper during his visit at ESAC.

References

Arav, N., Barlow, T. A., Laor, A., & Blandford, R. D. 1997, MNRAS, 288, 1015
Armentrout, B. K., Kraemer, S. B., & Turner, T. J. 2007, ApJ, 665, 237
Behar, E., Rasmussen, A. P., Blustin, A. J., et al. 2003, ApJ, 598, 232
Bianchi, S., Matt, G., Haardt, F., et al. 2001, A&A, 376, 77
Bianchi, S., Miniutti, G., Fabian, A. C., & Iwasawa, K. 2005, MNRAS, 360, 380
Bianchi, S., Guainazzi, M., & Chiaberge, M. 2006, A&A, 448, 499
Blustin, A. J., Page, M. J., Fuerst, S. V., Branduardi-Raymont G., & Ashton C. E. 2005, A&A, 431, 111
Boroson, T. A., & Green, R. F. 1992, ApJS, 80, 109
Cash, W. 1979, ApJ, 228, 939
Crenshaw, D. M., Kraemer, S. B., & George, I. M. 2003, ARA&A, 41, 117
Crummy, J., Fabian, A. C., Gallo, L., & Ross, R. R. 2006, MNRAS, 365, 1067
den Herder, J. W., Brinkman, A. C., Kahn, S. M., et al. 2001, A&A, 365, 7
Dickey, J. M., & Lockman, F. J. 1990, ARA&A, 28, 215
Ferland, G. J., Korista, K. T., Verner, D. A., et al. 1998, PASP, 110, 761
George, I. M., Turner, T. J., Netzer, H., et al. 1998, ApJS, 114, 73
Gondoin, P., Orr, A., Lumb, D., & Santos-Lleo, M. 2002, A&A, 388, 74
Grupe, D., Komossa, S., & Gallo, L. C. 2007, ApJ, 668, 111
Grupe, D., Komossa, S., Gallo L., et al. 2008, ApJ, accepted
Guainazzi, M., & Bianchi, S. 2007, MNRAS, 374, 1290
Kahn, S. M., Leutenegger, M. A., Cottam, J., et al. 2001, A&A, 365, 312
Kinkhabwala, A., Sako, M., Behar, E., et al. 2002, ApJ, 575, 732
Korista, K., Ferland, G., & Baldwin, J. 1997, ApJ, 487, 555
Krongold, Y., Nicastro, F., Elvis, M., et al. 2007, ApJ, 659, 1022
Larsson, J., Miniutti, G., Fabian, A. C., et al. 2007, [arXiv:0712.1906]
Longinotti, A. L., Sim, S. A., Nandra, K., & Cappi, M. 2007, MNRAS, 374, 237
Mason, K. O., Breevedl, A., Much, R., et al. 2001, A&A, 365, L36
Mewe, R., & Schrijver, J. 1978, A&A, 65, 99
Nandra K., & Pounds K. A. 1994, MNRAS, 268, 405
Netzer, H., Chelouche, D., George, I. M., et al. 2002, ApJ, 571, 256
Netzer, H., Kaspi, S., Behar, E., et al. 2003, ApJ, 599, 933
O'Neill, P. M., Nandra, K., Cappi, M., Longinotti, A. L., & Sim, S. A. 2007, MNRAS, 381, L94
Piconcelli, E., Jimenez-Bailón, E., Guainazzi, M., et al. 2005, A&A, 432, 15
Peterson, B. M., Ferrarese, L. Gilbert, K.-M., et al. 2004, ApJ, 613, 682
Porquet, D., & Dubau, J. 2000, A&AS, 143, 495
Porter, R. L., & Ferland, G. J. 2007, ApJ, 664, 586
Pounds, K. A., Reeves, J. N., King, A. R., & Page, K. L. 2004, MNRAS, 350, 10
Reynolds, C. S. 1997, MNRAS, 286, 513
Strüder, L., Briel, U., Dennerl, K., et al. 2001, A&A, 365, 18
Turner, T. J., & Pounds, K. A. 1989, MNRAS, 240, 833
Turner, T. J., Nandra, K., Zdziarsky, A. A., et al. 1993a, ApJ, 407, 556
Turner, T. J., George, I. M., & Mushotzky, R. F. 1993b, ApJ, 412, 72
Woo, J.-H., & Urry, C. M. 2002, ApJ, 579, 530